Acta Cryst. (1977). A**33**, 865–872

The Differential Geometry of Grain Boundaries: Tilt Boundaries

BY M. J. MARCINKOWSKI

Engineering Materials Group and Department of Mechanical Engineering, University of Maryland, College Park, Maryland 20742, *USA*

(*Received* 7 *February* 1977; *accepted* 31 *May* 1977)

A differential geometric analysis has been made of the various tensor quantities associated with a grain boundary. It is shown how these tensor quantities can be developed so as to give a unique and generalized formulation for the description of the dislocation content of such boundaries.

Introduction

In an earlier study (Marcinkowski & Sadananda, 1975), it was shown that the continuum theory of grain boundaries was compatible with the coincidence-site-lattice model. This formulation, however, was somewhat limited mathematically. It is therefore the purpose of the present analysis to formulate the continuum theory of grain boundaries in terms of the more general concepts of differential geometry. Kröner (1958), Bilby (1960) as well as Kondo (1955) have shown that the utilization of the highly developed methods of differential geometry are well suited to the treatment of lattice defects.

Distortion tensor associated with a grain boundary

Consider the formation of the symmetric tilt boundary shown in Fig. 1. In particular, the boundary may be viewed as being constructed by going through a series of well-defined stages or states (Kröner, 1958; Kondo, 1955; de Wit, 1968). The initial state, which will be denoted by capital Latin letters such as K, L, M, *etc.*, may be viewed as an ideal perfect crystal as shown in Fig. 1(*a*). The crystal may then be cut along the vertical dashed line into two regions labeled as #1 and #2 followed by rigid rotations to give the results shown in Fig. 1(*b*). This may be referred to as the torn state and will be designated by lower-case Latin letters k, l, m, *etc.* The grain boundary, or final state, shown in Fig. 1(*c*) may be formed from the torn state by the addition of wedges of extra matter to the latter state. An alternative method of formation would involve simple shears of opposite sign within each grain. The final state will be designated by Greek letters such as κ, λ, μ, *etc.* In a similar manner to that shown in Fig. 1, an asymmetric grain boundary may be created by the process shown in Fig. 2. A set of base vectors $\mathbf{e}_K$, $\mathbf{e}_k$ and $\mathbf{e}_\kappa$ may also be associated with each of the various grains.

The components of length dx^K and dx^k associated with the (K) and (k) states respectively may be related to one another as follows (Kröner, 1959):

$$dx^k = \mathbf{A}^k_K dx^K \tag{1a}$$

and

$$dx^K = \mathbf{A}^K_k dx^k \tag{1b}$$

etc., where the quantities $\mathbf{A}^k_K$ and $\mathbf{A}^K_k$ are termed the distortions. The distortion tensor connecting the (K) and (k) states of Fig. 1 may be written as

$$\mathbf{A}^k_K = \{\underset{1}{\mathbf{A}^k_K} H(-x^1_K)\}_1 + \{\underset{2}{\mathbf{A}^k_K} H(+x^1_K)\}_2 \tag{2}$$

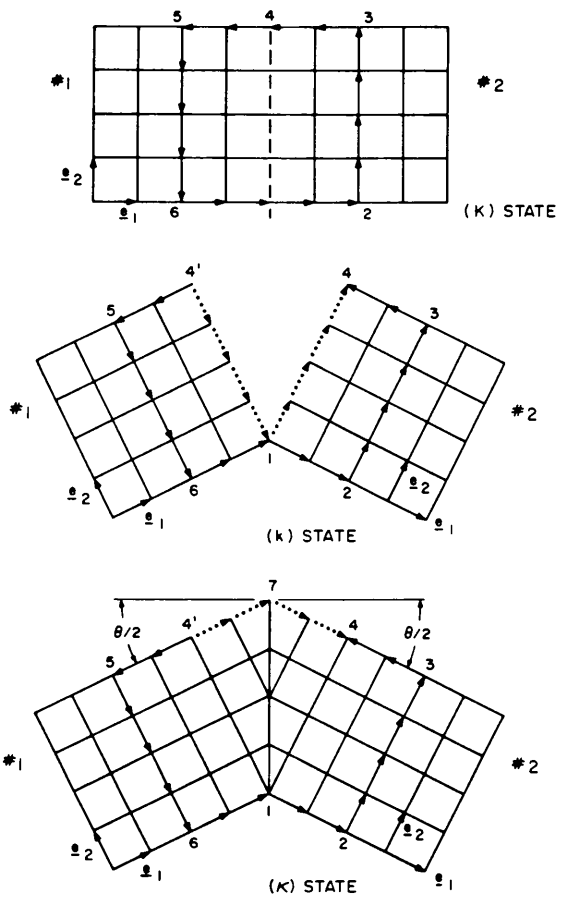

Fig. 1. Steps illustrating the formation of a symmetric tilt boundary: (*a*) initial reference state, (*b*) torn state, (*c*) dislocated state.

where $\underset{1}{\mathbf{A}}{}^{k}_{K}$ and $\underset{2}{\mathbf{A}}{}^{k}_{K}$ are simply the distortions within grains #1 and #2 respectively. Since the coordinates are simply dragged by the rigid rotations (Schouten, 1954), *i.e.*

$$dx^k = \delta^k_K dx^K, \tag{3}$$

where δ^k_K is the Kronecker delta, it follows that

$$\underset{1}{\mathbf{A}}{}^{k}_{K} = \underset{2}{\mathbf{A}}{}^{k}_{K} = \delta^k_K. \tag{4}$$

The quantities $H(-\underset{K}{x}{}^1)$ and $H(+\underset{K}{x}{}^1)$ in (2) are Heaviside functions defined by (Kröner, 1958; de Wit, 1973)

$$H(-\underset{K}{x}{}^1) = \begin{cases} 0 & \text{if } \underset{K}{x}{}^1 > 0 \\ 1 & \text{if } \underset{K}{x}{}^1 < 0 \end{cases} \tag{5a}$$

and

$$H(+\underset{K}{x}{}^1) = \begin{cases} 0 & \text{if } \underset{K}{x}{}^1 < 0 \\ 1 & \text{if } \underset{K}{x}{}^1 > 0 \end{cases} \tag{5b}$$

where the $\underset{K}{x}{}^1$ are measured with respect to a set of local coordinates in the (K) state of the potential boundary in Fig. 1(*a*). Thus, at the boundary, $\underset{K}{x}{}^1 = 0$, while within grain #1 it is negative, and positive within grain #2. Also important in (2) is that the quantities associated with grains #1 and #2 are separated by curly brackets. This is to emphasize that each of the two grains may be treated separately. The significance of this separation will become more clear as the present analysis is developed further in the following sections.

For the final state of the symmetric tilt boundary shown in Fig. 1(*c*) we may again write, similar to (2)

$$\mathbf{A}^{\kappa}_{K} = \{\underset{1}{\mathbf{A}}{}^{\kappa}_{K} H(-\underset{K}{x}{}^1)\}_1 + \{\underset{2}{\mathbf{A}}{}^{\kappa}_{K} H(+\underset{K}{x}{}^1)\}_2 \tag{6}$$

where

$$\underset{1}{\mathbf{A}}{}^{\kappa}_{K} = \begin{pmatrix} 1 & 0 & 0 \\ \tan\theta/2 & 1 & 0 \\ 0 & 0 & 1 \end{pmatrix} \tag{7a}$$

while

$$\underset{2}{\mathbf{A}}{}^{\kappa}_{K} = \begin{pmatrix} 1 & 0 & 0 \\ -\tan\theta/2 & 1 & 0 \\ 0 & 0 & 1 \end{pmatrix} \tag{7b}$$

where the last two distortions correspond to simple plastic shears which allow the gap in the (k) state to be filled up.

The asymmetric distortion giving rise to Fig. 2(*b*) can be written as

$$\mathbf{A}^{k^1}_{K^1} = \{\underset{1}{\mathbf{A}}{}^{k^1}_{K^1} H(-\underset{K^1}{x}{}^1)\}_1 + \{\underset{2}{\mathbf{A}}{}^{k^1}_{K^1} H(+\underset{K^1}{x}{}^1)\}_2 \tag{8}$$

where

$$\underset{1}{\mathbf{A}}{}^{k^1}_{K^1} = \underset{2}{\mathbf{A}}{}^{k^1}_{K^1} = \delta^{k^1}_{K^1}. \tag{9}$$

With respect to the (κ^1) state distortion of Fig. 2(*c*), we may write

$$\mathbf{A}^{\kappa^1}_{K^1} = \{\underset{1}{\mathbf{A}}{}^{\kappa^1}_{K^1} H(-\underset{K^1}{x}{}^1)\}_1 + \{\underset{2}{\mathbf{A}}{}^{\kappa^1}_{K^1} H(+\underset{K^1}{x}{}^1)\}_2 \tag{10}$$

where

$$\underset{1}{\mathbf{A}}{}^{\kappa^1}_{K^1} \equiv \underset{1}{\mathbf{A}}{}^{\kappa}_{K} \tag{11a}$$

while

$$\underset{2}{\mathbf{A}}{}^{\kappa^1}_{K^1} = \begin{pmatrix} 1 & 0 & 0 \\ 0 & \dfrac{1}{\cos\theta/2} & 0 \\ 0 & 0 & 1 \end{pmatrix}. \tag{11b}$$

The A^2_2 component in the last relation accounts for the plastic distortion which increases the length along the $\mathbf{x}^2$ direction of grain #2 in Fig. 2(*c*).

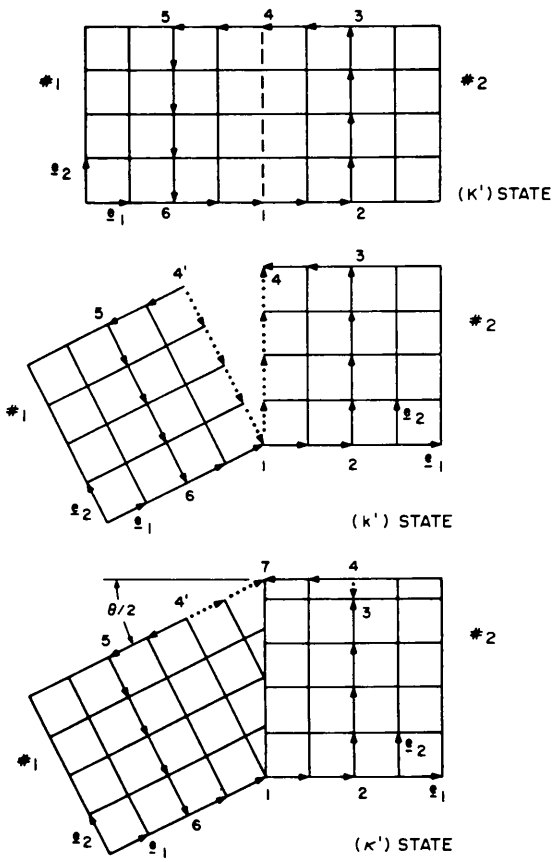

Fig. 2. Steps illustrating the formation of an asymmetric tilt boundary: (*a*) initial state, (*b*) torn state, (*c*) dislocated state.

Burgers circuit associated with a grain boundary

Fig. 1(*a*) shows a Burgers circuit 1–2–3–4–5–6–1 taken about a closed path in a counterclockwise direction. The corresponding circuit associated with the torn state is shown in Fig. 1(*b*). It is apparent that the latter Burgers circuit possesses closure failures associated with the pair of newly created surfaces given by the lengths 4′–1 and 1–4 which are shown by dotted arrows. The corresponding closure failures for the (κ) state are shown by the vectors 4′–7 and 7–4.

Fig. 3 shows a more detailed description of the

symmetric grain boundary illustrated in Fig. 1(*c*) (Marcinkowski & Sandananda, 1975). The boundary is shown by the vertical dotted line, while the open circles are coincidence sites common to both grains. The edge-type dislocations associated with the boundary are represented in heavy outline by their standard symbols. In addition, a Burgers circuit, identical to that shown in Fig. 1(*c*) is also drawn. Similarly, Fig. 4 shows the dislocation content and Burgers circuit associated with the asymmetric grain boundary illustrated in Fig. 2(*c*), but redrawn so as to encompass an integral number of lattice sites.

We are now in a position to examine the mathematical significance of the Burgers circuits discussed above.

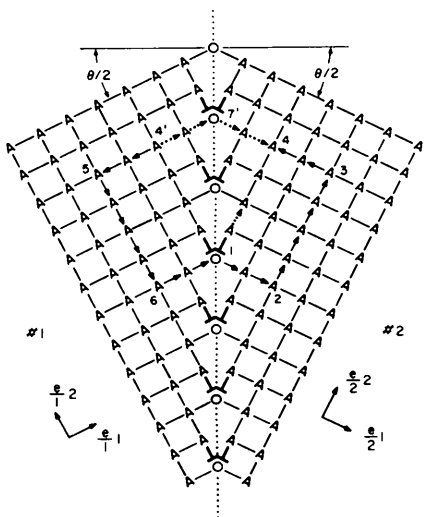

Fig. 3. Dislocation content and Burgers circuit associated with the 53·1° symmetric tilt boundary shown in Fig. 1(*c*).

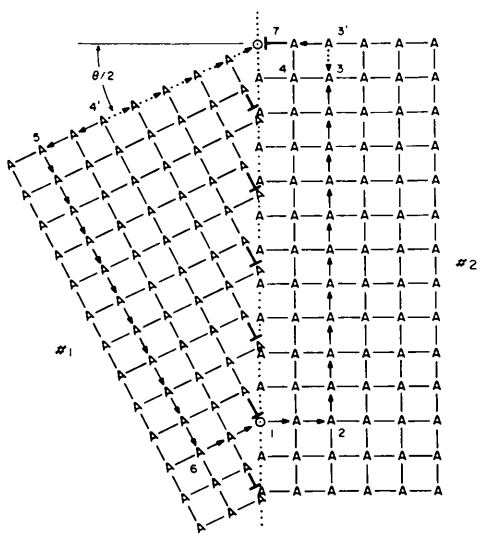

Fig. 4. Dislocation content and Burgers circuit associated with the 26·55 asymmetric tilt boundary shown in Fig. 2(*c*).

In particular, the Burgers vector of the (κ) state may be expressed by the following line integral:

$$\mathbf{b}^{\kappa} = -\oint \mathbf{A}^{\kappa}_{K} dx^{K} \tag{12}$$

where the above integral must be taken about a circuit in the (K) state as shown in Fig. 1(*a*). Applying the above integral to Fig. 1(*c*), in conjunction with (6) gives

$$\underset{\kappa}{b}{}^{1} = \{-A^{1}_{1}\Delta x^{2}_{5-6}\}_{1} + \{-A^{1}_{2}\Delta x^{2}_{2-3}\}_{2} \tag{13a}$$

where Δx^{2}_{5-6} *etc.* are simply the distances from 5 to 6, *etc.* in Fig. 1(*a*). Equation (13*a*) can be rewritten as

$$\underset{\kappa}{b}{}^{1} = \{4\tan\theta/2\}_{1} + \{4\tan\theta/2\}_{2}, \tag{13b}$$

or in terms of Fig. 1(*c*)

$$\underset{\kappa}{b}{}^{1} = \{\Delta x^{1}_{4'-7}\}_{1} + \{\Delta x^{1}_{7-4}\}_{2}. \tag{13c}$$

Procedures similar to that used for the (κ) state can also be applied to the (k) state of Fig. 1(*b*). However, we must first modify (12) to read

$$\mathbf{b}^{k} = \oint \mathbf{A}^{k}_{K} dx^{K}, \tag{14}$$

which with the aid of (2) gives

$$\underset{k}{b}{}^{2} = \{A^{2}_{1}\Delta x^{2}_{5-6}\}_{1} + \{A^{2}_{2}\Delta x^{2}_{2-3}\}_{2} \tag{15a}$$

or

$$\underset{k}{b}{}^{2} = \{-4\}_{1} + \{4\}_{2}. \tag{15b}$$

In terms of Fig. 1(*b*), the above equation becomes

$$\underset{k}{b}{}^{2} = \{\Delta x^{2}_{4'-1}\}_{1} + \{\Delta x^{2}_{1-4}\}_{2}. \tag{15c}$$

The closure failure $\underset{\kappa}{b}{}^{1}$ may be thought of as due to internal dislocations such as those depicted in Fig. 3, while $\underset{k}{b}{}^{2}$ measures the amount of new surface created by the tearing operation. We shall have more to say about these very important concepts later.

It is now a simple matter to extend the previous analysis to the asymmetric boundary of Fig. 2(*c*) or Fig. 4. Let us begin by rewriting (12) as

$$\mathbf{b}^{\kappa'} = -\oint \mathbf{A}^{\kappa'}_{K'} dx^{K'}, \tag{16}$$

which together with the distortions of (10) gives

$$\underset{\kappa'}{b}{}^{2} = \{-A^{2}_{1}\Delta x^{2}_{5-6}\}_{1} + \{-A^{2}_{2}\Delta x^{2}_{2-3}\}_{2} \tag{17a}$$

and

$$\underset{\kappa'}{b}{}^{1} = \{-A^{1}_{1}\Delta x^{2}_{5-6}\}_{1} + \{0\}_{2}, \tag{17b}$$

which in terms of Fig. 4 can be written more explicitly as

$$\underset{\kappa'}{b}{}^{2} = \{10\}_{1} + \left\{-\frac{10}{\cos\theta/2}\right\}_{2} = -\{1\}_{2} \tag{18a}$$

and

$$\underset{\kappa'}{b}{}^{1} = \{10\tan\theta/2\}_{1} + \{0\}_{2} \tag{18b}$$

or alternatively as

$$\underset{\kappa^1}{b}{}^2 = \{\underset{6-5}{\Delta x}{}^2\}_1 + \{\underset{3'-2}{\Delta x}{}^2\}_2 = \{\underset{3'-3}{\Delta x}{}^2\}_2 \tag{19a}$$

and

$$\underset{\kappa^1}{b}{}^1 = \{\underset{4'-7}{\Delta x}{}^1\}_1 + \{0\}_2. \tag{19b}$$

The torn (k^1) state of Fig. 2(*b*), similar to that of the (k) state gives rise to the following closure failure:

$$\mathbf{b}^{k^1} = \oint \mathbf{A}^{k^1}_{K^1} \mathrm{d}x^{k^1}, \tag{20}$$

which when used with (8) yields

$$\underset{k^1}{b}{}^2 = \{-4\}_1 + \{4\}_2, \tag{21}$$

i.e. the same result as that given by (15) for the (k) state. It should also be noted at this point that in the construction of Fig. 2(*c*), the distance 1–7 is less than unity. This does not alter the validity of the above equations; however, the drawback in this case is that the Burgers vector does not involve an integral number of interatomic jumps, and is thus somewhat inconvenient to construct. In simple physical terms then, we note that the net Burgers vector associated with a grain boundary, expressed in terms of crystal-lattice dislocations, is nothing more than the extra number of interatomic jumps between equivalent directions in the two adjacent grains, *i.e.* 4′–7–4 in the case of Fig. 3, and 4′–7 and 3′–3 in Fig. 4 (Marcinkowski & Sadananda, 1975).

The line integral of (12) can be converted into a surface integral by means of Stokes's theorem as follows (Schouten, 1951):

$$\mathbf{b}^\kappa = -\oint \mathbf{A}^\kappa_K \mathrm{d}x^K = -\int_s \partial_{[L} \mathbf{A}^\kappa_{K]} \mathrm{d}F^{LK} \tag{22}$$

where

$$\mathbf{b}^\kappa = -\int_s \partial_{[L} \mathbf{A}^\kappa_{K]} \mathrm{d}F^{LK} = -\int_s \tfrac{1}{2}[\partial_L \mathbf{A}^\kappa_K - \partial_K \mathbf{A}^\kappa_L] \mathrm{d}F^{LK}. \tag{23}$$

In the case of Fig. 1(*c*), (22) gives

$$\underset{\kappa}{b}{}^1 = \left\{ -\int_s \partial_1 A^1_2 \mathrm{d}F^{12} \right\}_1 + \left\{ -\int_s \partial_1 A^1_2 \mathrm{d}F^{12} \right\}_2 \tag{24a}$$

since $\mathrm{d}F^{12} = -\mathrm{d}F^{21} = \mathrm{d}x^1 \mathrm{d}x^2$. With the distortions given by (6), (24*a*) becomes

$$\underset{\kappa}{b}{}^1 = \left\{ \tan\theta/2 \int_{-\infty}^{+\infty} \underset{K}{\delta}(x^1) \mathrm{d}x^1 \int \mathrm{d}\underset{K}{x}{}^2 \right\}_1 + \left\{ \tan\theta/2 \int_{-\infty}^{+\infty} \underset{K}{\delta}(x^1) \mathrm{d}x^1 \int \mathrm{d}\underset{K}{x}{}^2 \right\}_2, \tag{24b}$$

where use has been made of the following relations (de Wit, 1973):

$$\partial_1 H(-\underset{K}{x}{}^1) = -\underset{K}{\delta}(x^1) \tag{25a}$$

and

$$\partial_1 H(+\underset{K}{x}{}^1) = +\underset{K}{\delta}(x^1), \tag{25b}$$

where $\underset{K}{\delta}(x^1)$ is the Dirac delta function defined such that it is zero everywhere for $\underset{K}{x}{}^1 \neq 0$ and which also has the following property:

$$\int_{-\infty}^{+\infty} \underset{K}{\delta}(x^1) \mathrm{d}\underset{K}{x}{}^1 = 1. \tag{26}$$

Since $\int \mathrm{d}\underset{K}{x}{}^2$ is simply equal to $\underset{2-3}{\Delta x}{}^2 = 4$ from Fig. 1(*a*), 24(*b*) reduces to

$$\underset{\kappa}{b}{}^1 = \{4 \tan\theta/2\}_1 + \{4 \tan\theta/2\}_2 \tag{27}$$

which is identical to that given by (13*b*). Equation (22*a*) can also be used in conjunction with the asymmetric tilt boundary of Fig. 4 and again gives results identical to those obtained by the use of (16). It is also possible to utilize an expression of the type given by (22*a*) for the (k) state. In particular

$$\mathbf{b}^k = \oint \mathbf{A}^k_K \mathrm{d}x^K = \int_s \partial_{[L} \mathbf{A}^k_{K]} \mathrm{d}F^{LK}. \tag{28}$$

This expression for the torn (k) and (k^1) states is identical to those given by (15) and (21) respectively.

Still a third way of expressing $\mathbf{b}^\kappa$ is by rewriting (23*b*) as

$$\mathbf{b}^\kappa = -\int \tfrac{1}{2} \mathbf{A}^L_\lambda \mathbf{A}^K_\mu [\partial_L \mathbf{A}^\kappa_K - \partial_K \mathbf{A}^\kappa_L] \mathrm{d}F^{\lambda\mu}, \tag{29a}$$

or in more concise form as

$$\mathbf{b}^\kappa = -\int_s \mathbf{S}_{\lambda\mu}{}^\kappa \mathrm{d}F^{\lambda\mu} \tag{29b}$$

where

$$\mathbf{A}^L_\lambda \mathbf{A}^\kappa_L = \delta^\kappa_\lambda \tag{30}$$

while the quantity $\mathbf{S}_{\lambda\mu}{}^\kappa$ is referred to as the torsion tensor (Schouten, 1954, 1951) given by

$$\mathbf{S}_{\lambda\mu}{}^\kappa = \tfrac{1}{2} \mathbf{A}^L_\lambda \mathbf{A}^K_\mu [\partial_L \mathbf{A}^\kappa_K - \partial_K \mathbf{A}^\kappa_L] \tag{31}$$

where it is apparent that $\mathbf{S}_{\lambda\mu}{}^\kappa$ is antisymmetric in the indices λ and μ. For the (κ) state of the symmetric boundary in Fig. 3, (31) gives for the specific component $\underset{\kappa}{S}{}_{1\dot{2}}{}^1$

$$\underset{\kappa}{S}{}_{1\dot{2}}{}^1 = \tfrac{1}{2}[A^1_1 A^2_2 - A^2_1 A^1_2] \partial_1 A^1_2. \tag{32a}$$

With the aid of (6) the above relation becomes

$$\underset{\kappa}{S}{}_{1\dot{2}}{}^1 = \{-\tfrac{1}{2} \tan\theta/2 \, \underset{\kappa}{\delta}(x^1)\}_1 + \{-\tfrac{1}{2} \tan\theta/2 \, \underset{\kappa}{\delta}(x^1)\}_2. \tag{32b}$$

When the above expression is substituted into (29*b*), we again obtain a result identical to that given by (27); thus establishing the self-consistency of the present formulation.

With respect to the asymmetric tilt boundary of Fig. 4, we may write, similar to (29*b*),

$$\mathbf{b}^{\kappa^1} = -\int_s \mathbf{S}_{\lambda^1\mu^1}{}^{\kappa^1} \mathrm{d}F^{\lambda^1\mu^1} \tag{33}$$

where it is easy to show that

$$S_{\underset{\kappa^1}{i}\,\underset{\kappa^1}{j}}{}^{1} = \{-\tfrac{1}{2}\tan\theta/2\,\delta(x^1_{\kappa^1})\}_1 + \{0\}_2 \qquad (34a)$$

and

$$S_{\underset{\kappa^1}{i}\,\underset{\kappa^1}{j}}{}^{2} = \{-\tfrac{1}{2}\delta(x^1_{\kappa^1})\}_1 + \{\tfrac{1}{2}\delta(x^1_{\kappa^1})\}_2, \qquad (34b)$$

which when substituted into (33) leads to the same results as that given by (18). In the case of the torn (k) and (k^1) states, (28) can be rewritten as

$$\mathbf{b}^k = \int_s \mathbf{\Omega}_{lm}{}^{k}\,\mathrm{d}F^{lm} \qquad (35a)$$

and

$$\mathbf{b}^{k^1} = \int_s \mathbf{\Omega}_{l^1 m^1}{}^{k^1}\,\mathrm{d}F^{l^1 m^1} \qquad (35b)$$

where the quantity $\mathbf{\Omega}_{lm}{}^{k}$ is termed the anholonomic object and may be written as (Schouten, 1954; Zorawski, 1967),

$$\mathbf{\Omega}_{lm}{}^{k} = \tfrac{1}{2}\mathbf{A}_l^L\mathbf{A}_m^M[\partial_L\mathbf{A}_M^k - \partial_M\mathbf{A}_L^k] \qquad (36)$$

with a similar expression for $\mathbf{\Omega}_{l^1 m^1}{}^{k^1}$. With the distortions associated with the affected coordinates, these can be evaluated to give

$$\Omega_{\underset{k}{i}\,\underset{k}{j}}{}^{2} = \{-\tfrac{1}{2}\delta(x^1_k)\}_1 + \{\tfrac{1}{2}\delta(x^1_k)\}_2 \qquad (37)$$

with an analogous expression existing for $\Omega_{\underset{k^1}{i}\,\underset{k^1}{j}}{}^{2}$. When substituted into (35), (37) gives the same results as those obtained from (15) and (21). We can conclude at this point that the torsion tensor $\mathbf{S}_{\lambda\mu}{}^{\kappa}$ may be viewed as a measure of the internal dislocation content within a crystal, while the anholonomic object $\mathbf{\Omega}_{lm}{}^{k}$ may be considered as a measure of the newly created free surface induced by the tearing process. There is, however, a close relation between the two quantities as we shall next see.

The (κ) state in Fig. 1(c) can be torn along the boundary (Kondo, 1962) which leads to the (κ^T) state shown in Fig. 5. The newly created free surfaces can be resolved into horizontal and vertical components. In this case we may write

$$\mathbf{b}^{\kappa^T} = -\oint \mathbf{A}_K^{\kappa^T}\,\mathrm{d}x^K \qquad (38a)$$

and

$$\mathbf{b}^{\kappa^T} = \oint \mathbf{A}_K^{\kappa^T}\,\mathrm{d}x^K \qquad (38b)$$

where $\mathbf{A}_K^{\kappa^T} \equiv \mathbf{A}_K^{\kappa}$. In terms of surface integrals, the above equations become

$$\mathbf{b}^{\kappa^T} = -\int_s \mathbf{S}_{\lambda^T\mu^T}{}^{\kappa^T}\,\mathrm{d}F^{\lambda^T\mu^T} \qquad (39a)$$

and

$$\mathbf{b}^{\kappa^T} = \int_s \mathbf{\Omega}_{\lambda^T\mu^T}{}^{\kappa^T}\,\mathrm{d}F^{\lambda^T\mu^T}. \qquad (39b)$$

In terms of Fig. 5, the first representation gives

$$b^1_{\kappa^T} = \{\Delta x^1_{4'-7}\}_1 + \{\Delta x^1_{7-4}\}_2, \qquad (40a)$$

while the second yields

$$b^1_{\kappa^T} = \{\Delta x^1_{1'-8}\}_1 + \{\Delta x^1_{1-8}\}_2. \qquad (40b)$$

It is apparent that the dislocation contribution to the Burgers circuit given by (40a) is just balanced by the free-surface contribution given by (40b). This also means that

$$\mathbf{S}_{\lambda^T\mu^T}{}^{\kappa^T} = \mathbf{\Omega}_{\lambda^T\mu^T}{}^{\kappa^T} \qquad (41)$$

so that we may write

$$\mathbf{b}^{\kappa^T} = -\int_s (\mathbf{S}_{\lambda^T\mu^T}{}^{\kappa^T} - \mathbf{\Omega}_{\lambda^T\mu^T}{}^{\kappa^T})\,\mathrm{d}F^{\lambda^T\mu^T} = 0. \qquad (42)$$

We thus see the close relation between the torsion tensor and the anholonomic object, and it is in fact this close relation which has enabled Zorawski (1967) to formulate his treatment of dislocations almost exclusively in terms of the latter quantity. The (κ^1) state of Fig. 2(c) can also be torn to generate a (κ^{1T}) state corresponding to that of (κ^T).

Interpretation of the various tensor quantities associated with a grain boundary

It has been shown that the torsion tensor given by (31) is a measure of the dislocation density (Kröner, 1958). This is most simply seen by writing (29b) in differential form as follows:

$$\mathrm{d}\mathbf{b}^{\kappa} = -\mathbf{S}_{\mu\lambda}{}^{\kappa}\mathrm{d}F^{\mu\lambda} = -\mathbf{S}_{\mu\lambda}{}^{\kappa}\boldsymbol{\varepsilon}^{\nu\mu\lambda}\mathrm{d}F_{\nu} = \boldsymbol{\alpha}^{\nu\kappa}\mathrm{d}F_{\nu} \qquad (43)$$

where $\boldsymbol{\alpha}^{\nu\kappa}$ is defined as the dislocation density given by

$$\boldsymbol{\alpha}^{\nu\kappa} = -\boldsymbol{\varepsilon}^{\nu\mu\lambda}\mathbf{S}_{\mu\lambda}{}^{\kappa} \qquad (44)$$

and where $\boldsymbol{\varepsilon}^{\nu\mu\lambda}$ is the permutation tensor defined by

$$\boldsymbol{\varepsilon}^{\nu\mu\lambda} = \mathbf{e}^{\nu\mu\lambda}/\sqrt{g} \qquad (45)$$

while $\mathbf{e}^{\nu\mu\lambda}$ are permutation symbols and g is the determinant of the metric tensor $\mathbf{g}_{\kappa\lambda}$. For the symmetric tilt boundary of Fig. 3, the only non-vanishing component associated with (44) may be written as

$$\alpha_{\kappa}^{31} = \{\tan\theta/2\,\delta(x^1_{\kappa})\}_1 + \{\tan\theta/2\,\delta(x^1_{\kappa})\}_2 \qquad (46a)$$

where (32b) has been utilized. In terms of Fig. 1(c), (46a) can be written as

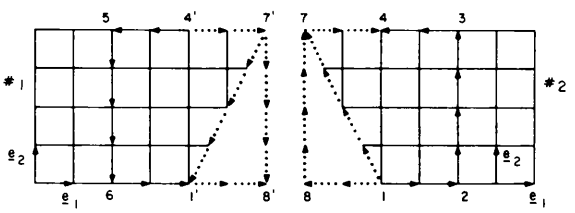

Fig. 5. Torn dislocated state of Fig. 1(c).

$$\underset{\kappa}{\alpha}^{31} = \left\{\frac{\Delta x^1}{\frac{4'-7}{1-4'}\,\Delta x^2}\right\}_1 + \left\{\frac{\Delta x^1}{\frac{7-4}{1-4}\,\Delta x^2}\right\}_2 . \tag{46b}$$

Note also in the symbol $\boldsymbol{\alpha}^{\nu\kappa}$, that ν refers to the direction of the dislocation line, and κ to the component of the Burgers vector. In the case of the dislocation density associated with the asymmetric boundary of Fig. 4, we have two components, which from (44) and (34), are given by

$$\underset{\kappa^1}{\alpha}^{31} = \{\tan\theta/2\ \delta(\underset{\kappa^1}{x^1})\}_1 + \{0\}_2 \tag{47a}$$

and

$$\underset{\kappa^1}{\alpha}^{32} = \{\delta(\underset{\kappa^1}{x^1})\}_1 + \{\delta(\underset{\kappa^1}{x^1})/\sqrt{g}\}_2 \equiv \{-\tfrac{1}{10}\}_2 \tag{47b}$$

since $g = 1/\cos(\theta/2) = 10/11$. In terms of Fig. 4

$$\underset{\kappa^1}{\alpha}^{31} = \left\{\frac{\Delta x^1}{\frac{4'-7}{1-4'}\,\Delta x^2}\right\}_1 + \{0\}_2 \tag{48a}$$

and

$$\underset{\kappa^1}{\alpha}^{32} = \left\{\frac{\Delta x^2}{\frac{1-4'}{1-4'}\,\Delta x^2}\right\}_1 + \left\{\frac{\Delta x^2}{\frac{3'-2}{2-3}\,\Delta x^2}\right\}_2 \equiv \left\{\frac{\Delta x^2}{\frac{3'-3}{2-3}\,\Delta x^2}\right\}_2 . \tag{48b}$$

In the case of the torn states we can write, similar to (44)

$$\boldsymbol{\alpha}^{nk} = \boldsymbol{\varepsilon}^{nml}\boldsymbol{\Omega}_{ml}{}^{\kappa} \tag{49}$$

which for Fig. 1(*b*) gives

$$\underset{k}{\alpha}^{32} = \{-\delta(\underset{k}{x^1})\}_1 + \{\delta(\underset{k}{x^1})\}_2 \tag{50a}$$

where (37) has been used. In terms of Fig. 1(*b*)

$$\underset{k}{\alpha}^{32} = \left\{\frac{\Delta x^2}{\frac{4'-1}{1-4'}\,\Delta x^2}\right\}_1 + \left\{\frac{\Delta x^2}{\frac{1-4}{1-4}\,\Delta x^2}\right\}_2 , \tag{50b}$$

with similar results holding for the (k^1) state. For the (κ^T) state of Fig. 5, it is easy to see that

$$\underset{S}{\boldsymbol{\alpha}}^{\nu T_\kappa T} = -\underset{\Omega}{\boldsymbol{\alpha}}^{\nu T_\kappa T} . \tag{51}$$

The expression given by (29*b*) is not the most generalized description for the closure failure associated with a given Burgers circuit. According to Kröner (1958), Kondo (1955), Schouten (1951, 1954), a more general equation is given by

$$\mathbf{b}^{\kappa} = -\int_S [\mathbf{S}_{\mu\lambda}{}^{\kappa} + \tfrac{1}{2}\mathbf{R}_{\mu\lambda\nu}{}^{\kappa}\mathbf{C}^{\nu}]\mathrm{d}F^{\mu\lambda} \tag{52}$$

where $\mathbf{R}_{\mu\lambda\nu}{}^{\kappa}$ is the Riemann–Christoffel curvature tensor given by

$$\mathbf{R}_{\mu\lambda\nu}{}^{\kappa} = 2\partial_{[\mu}\boldsymbol{\Gamma}^{\mu}_{\lambda]\nu} + 2\boldsymbol{\Gamma}^{\kappa}_{[\mu|\rho|}\boldsymbol{\Gamma}^{\rho}_{\lambda]\nu} \tag{53a}$$

or equivalently as

$$\mathbf{R}_{\mu\lambda\nu}{}^{\kappa} = \partial_{\mu}\boldsymbol{\Gamma}^{\kappa}_{\lambda\nu} - \partial_{\lambda}\boldsymbol{\Gamma}^{\kappa}_{\mu\nu} + \boldsymbol{\Gamma}^{\kappa}_{\mu\rho}\boldsymbol{\Gamma}^{\rho}_{\lambda\nu} - \boldsymbol{\Gamma}^{\kappa}_{\lambda\rho}\boldsymbol{\Gamma}^{\rho}_{\mu\nu}, \tag{53b}$$

where $\boldsymbol{\Gamma}^{\kappa}_{\mu\lambda}$ are referred to as the coefficients of connection expressed by

$$\boldsymbol{\Gamma}^{\kappa}_{\mu\lambda} = \left\{{}^{\kappa}_{\mu\lambda}\right\} + \mathbf{T}_{\mu\lambda}{}^{\kappa}, \tag{54}$$

where $\left\{{}^{\kappa}_{\mu\lambda}\right\}$ are Christoffel symbols of the second kind defined by

$$\left\{{}^{\kappa}_{\mu\lambda}\right\} = \tfrac{1}{2}\mathbf{g}^{\kappa\sigma}(\partial_{\mu}\mathbf{g}_{\lambda\sigma} + \partial_{\lambda}\mathbf{g}_{\mu\sigma} - \partial_{\sigma}\mathbf{g}_{\mu\lambda}) \tag{55}$$

while

$$\mathbf{T}_{\mu\lambda}{}^{\kappa} = \mathbf{S}_{\mu\lambda}{}^{\kappa} - \mathbf{S}_{\lambda\cdot\mu}^{\ \ \kappa} + \mathbf{S}^{\kappa}_{\cdot\mu\lambda} \tag{56}$$

where

$$\mathbf{S}_{\lambda\cdot\mu}^{\ \ \kappa} = \mathbf{g}_{\mu\sigma}\mathbf{g}^{\kappa\rho}\mathbf{S}_{\lambda\rho}{}^{\sigma} \tag{57a}$$

while

$$\mathbf{S}^{\kappa}_{\cdot\mu\lambda} = \mathbf{g}_{\lambda\sigma}\mathbf{g}^{\kappa\rho}\mathbf{S}_{\rho\mu}{}^{\sigma} . \tag{57b}$$

For the symmetric grain boundary of Fig. 3, (55) gives

$$\left\{{}^{1}_{12}\right\}_{\kappa} = \{\tfrac{1}{2}g^{12}\partial_1 g_{22}\}_1 + \{\tfrac{1}{2}g^{12}\partial_1 g_{22}\}_2, \tag{58}$$

which, since g_{22} is constant, gives

$$\left\{{}^{1}_{12}\right\}_{\kappa} = \{0\}_1 + \{0\}_2 . \tag{59}$$

Since $\left\{{}^{\kappa}_{\mu\lambda}\right\}$ is symmetric in μ and λ, the same result holds for $\left\{{}^{1}_{21}\right\}_{\kappa}$. Next, with the aid of (56) and (57), we obtain

$$T_{\dot{1}\dot{2}}{}^{1} = S_{\dot{1}\dot{2}}{}^{1} - S_{\dot{2}\dot{1}}{}^{1} + 0 = 2S_{\dot{1}\dot{2}}{}^{1} \tag{60a}$$

and

$$T_{\dot{2}\dot{1}}{}^{1} = S_{\dot{2}\dot{1}}{}^{1} - 0 + S_{\dot{1}\dot{2}}{}^{1} = 0. \tag{60b}$$

Thus, from (54)

$$\underset{\kappa}{\Gamma}{}^{1}_{12} = \{\Gamma^{1}_{12}\}_1 + \{\Gamma^{1}_{12}\}_2 = \{2S_{\dot{1}\dot{2}}{}^{1}\}_1 + \{2S_{\dot{1}\dot{2}}{}^{1}\}_2 \tag{61a}$$

while

$$\underset{\kappa}{\Gamma}{}^{1}_{21} = \{\Gamma^{1}_{21}\}_1 + \{\Gamma^{1}_{21}\}_2 = \{0\}_1 + \{0\}_2 . \tag{61b}$$

Now for $\underset{\kappa}{b}{}^{1}$ given by (52), the only possible components of $\mathbf{R}_{\dot{\mu}\dot{\lambda}\dot{\nu}}{}^{\kappa}$ are $R_{\dot{1}\dot{2}\dot{2}}{}^{1}$, $R_{\dot{2}\dot{1}\dot{2}}{}^{1}$, $R_{\dot{1}\dot{2}\dot{1}}{}^{1}$ and $R_{\dot{2}\dot{1}\dot{1}}{}^{1}$. From (53*b*) it is a simple matter to show that they all vanish. This result has a number of important implications. In the first place, it shows that (52) for grain boundaries reduces to the simple expression for the Burgers vector given by (29*b*). Secondly, it shows that the space associated with Fig. 3 is one of absolute parallelism, *i.e.* where parallel displaced vectors are independent of path (Kunin, 1965). More specifically stated, this means that the only sources of distortion are dislocations.

An analysis similar to that given above can next be carried out for the antisymmetric boundary shown in Fig. 4. In particular, we obtain

$$\underset{\kappa^1}{\Gamma}{}^{1}_{12} = \{2S_{\dot{1}\dot{2}}{}^{1}\}_1 + \{0\}_2 \tag{62a}$$

and

$$\underset{\kappa^1}{\Gamma}{}^{1}_{21} = \{0\}_1 + \{0\}_2 \tag{62b}$$

while

$$\underset{\kappa^1}{\Gamma}{}^{2}_{12} = \{2S_{\dot{1}\dot{2}}{}^{2}\}_1 + \{2S_{\dot{1}\dot{2}}{}^{2}\}_2 \tag{63a}$$

and

$$\underset{\kappa^1}{\Gamma}{}^{2}_{21} = \{0\}_1 + \{0\}_2 . \tag{63b}$$

Having determined the coefficients of connection for both the symmetric and asymmetric grain boundaries, it is next possible to express the Burgers vectors

of these boundaries in still a fourth way by use of the concept of parallel displacement of a vector $\mathbf{c}^\lambda$ through a distance dx^μ. According to Kröner (1959) and Schouten (1954) the resulting vector difference $d\mathbf{c}^\kappa$ occasioned by such a displacement is given by

$$d\mathbf{c}^\kappa = -\mathbf{\Gamma}^\kappa_{\mu\lambda}\mathbf{c}^\lambda dx^\mu, \tag{64}$$

which is seen to be equivalent to (29*b*) when it is realized that $\mathbf{c}^\lambda = \int dx^\lambda$. For the symmetric tilt boundary, the above equation gives

$$\underset{\kappa}{dc^1} = -\Gamma^1_{12}c^2 dx^1, \tag{65a}$$

which from (69*a*) and (37*b*) gives

$$\underset{\kappa}{\Delta c^1} = \{4\tan\theta/2\}_1 + \{4\tan\theta/2\}_2 \tag{65b}$$

where c^2 has been taken as 4. Again, this is simply the identical result given by (27). In physical terms, (64) shows the manner in which the vector $\underset{\kappa}{c^2} = \underset{6-5}{\Delta x^2}$ changes at the boundary as it is displaced by parallel transport in the deformed space along the direction $\underset{\kappa}{\Delta x^1} \equiv \underset{6-1-2}{\Delta x^1}$. Equation (64) can also be used to obtain a set of equations for the asymmetric tilt boundary of Fig. 4 as well as for the torn (k) and (k^1) states.

Uniqueness of the Burgers circuit associated with a grain boundary

We next turn our attention to some important questions concerning the uniqueness of the dislocation content associated with the grain boundaries discussed thus far. In particular, Fig. 6 shows a symmetric tilt boundary in which the atom arrangement at the boundary is identical to that given in Fig. 3. The distortions associated with both grains, as well as the dislocation content of the boundary however, are seen to be completely different in both cases. In particular, we must now alter (7) as follows:

$$\underset{1}{\mathbf{A}^\kappa_K} = \begin{pmatrix} 1 & 0 & 0 \\ -\tan\left(\dfrac{\pi-\theta}{2}\right) & 1 & 0 \\ 0 & 0 & 1 \end{pmatrix} = \begin{pmatrix} 1 & 0 & 0 \\ -\cot\left(\dfrac{\theta}{2}\right) & 1 & 0 \\ 0 & 0 & 1 \end{pmatrix}, \tag{66a}$$

while

$$\underset{2}{\mathbf{A}^\kappa_K} = \begin{pmatrix} 1 & 0 & 0 \\ \tan\left(\dfrac{\pi-\theta}{2}\right) & 1 & 0 \\ 0 & 0 & 1 \end{pmatrix} = \begin{pmatrix} 1 & 0 & 0 \\ \cot\left(\dfrac{\theta}{2}\right) & 1 & 0 \\ 0 & 0 & 1 \end{pmatrix}. \tag{66b}$$

With the use of (12), it is easy to show that

$$\underset{\kappa}{b^1} = \{-A^1_2 \underset{5-6}{\Delta x^2}\}_1 + \{-A^1_2 \underset{2-3}{\Delta x^2}\}_2 \tag{67a}$$

which upon substitution of (66) gives

$$\underset{\kappa}{b^1} = \{-2\cot\theta/2\}_1 + \{-2\cot\theta/2\}_2. \tag{67b}$$

A factor of 2 now appears in the above equation rather than 4, as was the case for (13*b*), because the reference lattice in the (K) state is now halved in length. In terms of Fig. 6, (67*b*) may be written as

$$\underset{\kappa}{b^1} = \{\underset{7-1}{\Delta x^1}\}_1 + \{\underset{1-7}{\Delta x^1}\}_2. \tag{67c}$$

For the torsion tensor associated with Fig. 6, on the other hand, (32*a*) gives

$$\underset{\kappa}{S_{i\,i}{}^1} = \{-\tfrac{1}{2}\cot\theta/2\,\delta(\underset{\kappa}{x^1})\}_1 + \{-\tfrac{1}{2}\cot\theta/2\,\delta(\underset{\kappa}{x^1})\}_2. \tag{68}$$

The above equation, used together with (44) yields

$$\underset{\kappa}{\alpha^{31}} = \{\cot\theta/2\,\delta(\underset{\kappa}{x^1})\}_1 + \{\cot\theta/2\,\delta(\underset{\kappa}{x^1})\}_2, \tag{69a}$$

which in terms of Fig. 6 is simply

$$\alpha^{31} = \begin{Bmatrix} \underset{7-1'}{\Delta x^1} \\ \underset{4-1'}{\Delta x^2} \end{Bmatrix}_1 + \begin{Bmatrix} \underset{1-7}{\Delta x^1} \\ \underset{4-1}{\Delta x^2} \end{Bmatrix}_2. \tag{69b}$$

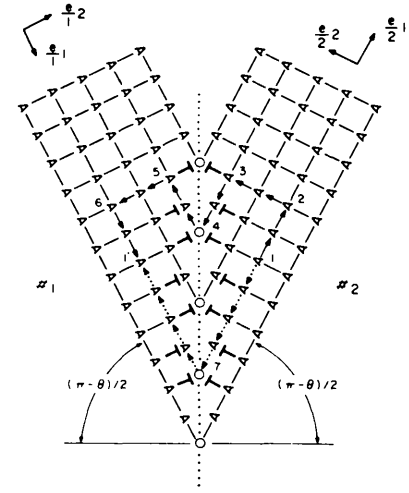

Fig. 6. Alternative description of the symmetric tilt boundary shown in Fig. 3.

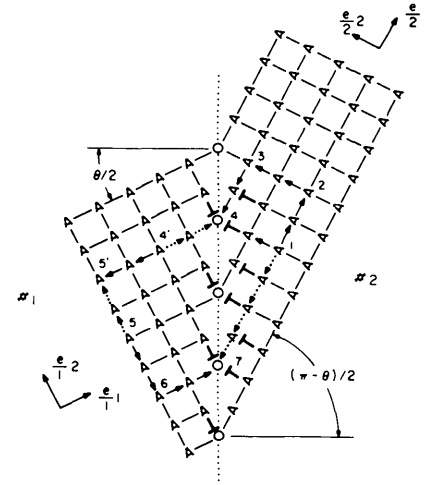

Fig. 7. Second alternative description of the symmetric tilt boundary shown in Fig. 3.

There are still two more alternative descriptions of the grain boundary shown in Fig. 3, one of which is shown in Fig. 7. In this particular circuit, grain #1 has the distortion associated with the boundary of Fig. 3, while grain #2 has the distortion associated with the boundary in Fig. 6. This boundary thus has associated with it still a third dislocation content in spite of the fact that the atom arrangements remain identical to those of Figs. 3 and 6. In particular,

$$b^1_\kappa = \{\Delta x^1_{4'-4}\}_1 + \{\Delta x^1_{1-7}\}_2, \tag{70a}$$

while

$$b^2_\kappa = \{\Delta x^2_{5-5'}\}_1 + \{0\}_2. \tag{70b}$$

Also important to note is that the closure failure component 5–5′ in Fig. 7 plays the same role as the component 3′–3 of the asymmetric boundary of Fig. 4. The above results are quite general and apply to low as well as high-angle boundaries. Also important to note is that the quantity $\tan(\theta/2)$ appears in many of the previous equations. This is not surprising in that it forms the basis for the coincidence-site-lattice description of grain boundaries (Marcinkowski & Sadananda, 1975; Marcinkowski, Sadananda & Tseng, 1973).

The present results at first appear quite surprising in that they show a different grain-boundary-dislocation content in spite of the fact that the atom arrangements within the boundary are identical. The above arguments would also seem to violate the principle that a dislocation is a state property and should be independent of the method of formation. However, the present theory may be thought of as global in nature in that it does not look at the individual nature of a dislocation in the grain boundary. Instead, it describes what type of wedges, or equivalently, simple shears must be imparted to each grain of the (K) state to generate the final state. This description is, of course, totally contained within the respective distortion tensors. The dislocation content in turn is described in terms of the number of extra half planes which comprise the extra wedge of material. In a sense, the present theory is a treatment of these extra half planes, and thus a more generalized theory than that required for grain boundaries above. This can be seen by reference to (46a) which shows that even for $\theta = \pi/2$, there is a dislocation density associated with such a boundary. Strictly speaking, however, this cannot be a grain boundary. However, from the point of view of the present theory, this result says that the final state is arrived at from the initial state by the insertion of a pair of 45° wedges into the (K) state. A more generalized theory to indicate when these 'perfect' boundaries occur would require the incorporation of the crystal symmetry into the present analysis.

Summary and conclusions

The techniques of differential geometry have been applied to the specific case of grain boundaries of both the symmetric and asymmetric types. Quantities such as the distortion tensor, lattice connection, curvature tensor, Burgers vector and dislocation density tensor all have well defined physical meanings with respect to such boundaries, and have been analyzed in detail in terms of the Burgers circuit.

The present research effort was carried out at the Institut für Theoretische und Angewandte Physik der Universität Stuttgart in the Federal Republic of Germany under a Senior US Scientist Award presented to the author by the Alexander von Humboldt Stiftung in conjunction with a one-year sabbatical leave. Financial support for the present study was also provided in part by the National Science Foundation under Grant No. DMR-7202944. The author is especially indebted to Professor Ekkehart Kröner for his kind assistance during the course of this investigation. The author would also like to express his thanks to Professor K. Sadananda of the Engineering Materials Group and the Department of Mechanical Engineering of the University of Maryland as well as to Dr R. de Wit of the Metallurgy Division and Institute for Materials Research of The National Bureau of Standards, Washington, DC, for numerous discussions dealing with the fundamental nature of dislocations.

References

BILBY, B. A. (1960). *Prog. Solid Mech.* **1**, 329–398.

KONDO, K. (1955). *Memoirs of the Unifying Study of the Basic Problems in Engineering Sciences by Means of Geometry*. Tokyo: Gakuyutsu Bunken Fukyu-kai.

KONDO, K. (1962). *RAAG Memoirs*, Vol. III, edited by K. KONDO, pp. 173–183. Tokyo: Gakuyutsu Bunken Fukyu-kai.

KRÖNER, E. (1958). *Kontinuumstheorie der Versetzungen und Eigenspannungen*. Berlin: Springer.

KRÖNER, E. (1959). *Arch. Ration. Mech. Anal.* **4**, 273–334.

KUNIN, I. A. (1965). *Methods of Tensor Analysis in the Theory of Dislocations*, Supplement to *Tensor Analysis for Physicists*, by J. A. SCHOUTEN, US Department of Commerce, Springfield, Virginia 22151.

MARCINKOWSKI, M. J. & SADANANDA, K. (1975). *Acta Cryst.* A**31**, 280–292.

MARCINKOWSKI, M. J., SADANANDA, K. & TSENG, WEN FENG (1973). *Phys. Stat. Sol.* (*a*), **17**, 423–433.

SCHOUTEN, J. A. (1951). *Tensor Analysis for Physicists*. Oxford: Clarendon Press.

SCHOUTEN, J. A. (1954). *Ricci-Calculus*. Berlin: Springer.

WIT, R. DE (1968). *Mechanisms of Generalized Continua*, edited by E. KRÖNER, pp. 251–261. New York: Springer.

WIT, R. DE (1973). *J. Res. Nat. Bur. Stand., A: Phys. Chem.* **77A**, 607–658.

ZORAWSKI, M. (1967). *Théorie Mathématique des Dislocations*. Paris: Dunod.